Induction by kainate of theta frequency rhythmic activity in the rat medial septum–diagonal band complex *in vitro*

Helen L. Garner, Miles A. Whittington and Zaineb Henderson

School of Biomedical Sciences, The Worsley Building, University of Leeds, Leeds LS2 9JT, UK

The medial septum–diagonal band (MSDB) complex, via the septohippocampal pathway, is thought to be critical for the generation and/or maintenance of the hippocampal theta rhythm *in vivo*. The aim was to determine whether the MSDB is capable of generating and maintaining its own rhythmic firing activity, a mechanism by which it could impose a theta frequency oscillatory activity on the hippocampus. Bath application of 50–300 nM kainate to an *in vitro* preparation of 20- to 25-day-old rat MSDB elicited rhythmic extracellular field activity primarily within the theta frequency band (4–12 Hz). This activity was observed both at 33°C and at 37°C, and was localized to the midline part of the MSDB that is rich in parvalbumin-containing neurones. The application of neurotransmitter receptor antagonists and putative gap junction blockers showed that the oscillatory field activity was dependent upon the activation of $GABA_A$ receptors and possibly gap junctions, but not on the activation of NMDA, $GABA_B$, muscarinic or nicotinic receptors. The frequency of the oscillatory activity was reduced by the application of diazepam or low doses of baclofen. Intracellular recording showed that concomitant action potential firing activity in putative GABAergic and cholinergic neurone populations was of a single spiking rather than a bursting firing nature, and was coherent with extracellularly recorded oscillatory field activity. We conclude that kainate activation of neuronal circuitry in the MSDB is capable of synchronization of rhythmic activity in the MSDB, and that this may underlie the mechanism for phase-locking rhythmic burst activity in the MSDB *in vivo*.

(Resubmitted 6 December 2004; accepted after revision 24 January 2005; first published online 27 January 2005)
Corresponding author Z. Henderson: School of Biomedical Sciences, The Worsley Building, University of Leeds, Leeds LS2 9JT, UK. Email: z.henderson@leeds.ac.uk

Rhythmic patterns of electrical activity have been recorded from cortical areas at various frequencies including theta (4–12 Hz), beta (20–30 Hz), gamma (40–80 Hz) and ultrafast (> 80 Hz) frequencies. Only recently have the important roles of this activity been evident in cognition and perception (Singer, 1999). Field potential oscillations at theta frequencies (4–12 Hz) are particularly prominent in the hippocampal formation in conscious or urethane-anaesthetized animals (Green & Arduini, 1954; Vanderwolf, 1969; Green & Rawlins, 1979). The hippocampal theta rhythm has been correlated with specific behaviours such as rapid eye movement (REM) sleep and various types of locomotive activities (Vanderwolf, 1969; Jouvet, 1969), and has been implicated in the processing of visuo-spatial information, and memory formation and retrieval (O'Keefe & Conway, 1978; Larson & Lynch, 1986; Buzsaki, 1989).

Lesion and stimulation studies indicate that the medial septal diagonal band complex (MSDB), via the septohippocampal pathway, plays a pivotal role in the generation and pacing of theta frequency oscillations in the hippocampus (reviewed by Stewart & Fox, 1990; Vinogradova, 1995). The predominant neuronal populations in the MSDB are cholinergic and GABAergic neurones (Gritti *et al.* 1993), and a significant proportion of the GABAergic cells contain the calcium-binding protein parvalbumin (Freund, 1989; Kiss *et al.* 1990). Both the cholinergic and GABAergic cells, including those that contain parvalbumin, project to the hippocampus via the dorsal fornix–fimbria pathway (Lewis *et al.* 1967; Kohler *et al.* 1984; Freund, 1989). The GABAergic cells possess myelinated axons and innervate the somata and dendrites of GABAergic hippocampal interneurones, whilst the cholinergic neurones have unmyelinated axons that synapse onto all hippocampal cell types (Frotscher & Leranth, 1986; Freund & Antal, 1988; Jones *et al.* 1999; Henderson *et al.* 2001). This organization of the septohippocampal pathway suggests that the MSDB

This work is dedicated to the memory of Professor E. H. Buhl.

DOI: 10.1113/jphysiol.2004.080622

GABAergic neurones have a phasic action on specific cell types, whilst the cholinergic neurones have a slower, tonic action on all cell types in the hippocampal formation.

A significant proportion of septohippocampal neurones display rhythmic bursting activity that is phase-locked with and tightly coupled to the frequency of the hippocampal theta rhythm during various behavioural states, and this is a property of both GABAergic and cholinergic neurones (Green & Arduini, 1954; Petsche *et al.* 1962; Gogolak *et al.* 1967; Apostol & Creutzfeldt, 1974; Lamour *et al.* 1984; Alonso *et al.* 1987; Sweeney *et al.* 1992; Brazhnik & Fox, 1997; King *et al.* 1998). The mechanisms that generate the rhythmic burst firing activity in the MSDB and determine its frequency, phase relation and synchrony are unclear, as is the nature of the contribution made by the rhythmic burst firing activity to the theta rhythm in the hippocampal formation. The interconnectivity between MSDB cells is believed to be critical for the rhythmic output from the septal complex (Stewart & Fox, 1990; Brazhnik & Fox, 1997). Morphological evidence of putative connections between the different cell types of the MSDB support this mechanistic hypothesis (Brauer *et al.* 1998; Henderson *et al.* 2001, 2004). Electrophysiological studies on the hippocampus *in vitro* and *in vivo* suggest that the production and synchronization of oscillatory activity at different frequencies in the hippocampus are attributed primarily to networks of GABAergic interneurones, connected via chemical and electrical synapses (Cobb *et al.* 1995; Whittington *et al.* 1995; Ylinen *et al.* 1995; Penttonen *et al.* 1998; Hormuzdi *et al.* 2001). The aim of this study, therefore, was to use an MSDB slice preparation to determine whether the MSDB *in vitro* is capable of producing a rhythmic output, in the absence of its connections with the hippocampus and other areas.

Methods

Preparation of brain slices

All procedures were carried out in accordance with the UK Animals (Scientific Procedures) Act 1986. Male Wistar rats ($n = 150$, 20–25 days postnatal) were anaesthetized with inhaled isoflurane (Baxter, Thetford, UK), followed by intraperitoneal injection of Sagatal (sodium pentobarbitone, 100 mg kg^{-1}, Rhône Mérieux Ltd, Harlow, UK). When all pedal reflexes were abolished, the rats were perfused intracardially with 50 ml chilled (5°C), oxygenated artificial cerebrospinal fluid (ACSF) in which the sodium chloride had been replaced by sucrose. This ACSF contained (mM): 252 sucrose, 3 KCl, 1.25 NaH_2PO_4, 24 $NaHCO_3$, 2 $MgSO_4$, 2 $CaCl_2$, 10 glucose. Up to three parasagittal slices (450 μm) of the brain containing the MSDB, and taken within 1 mm of the midline, were cut at 4–5°C in the same ACSF using a Leica VT1000S vibratome (Leica Microsystems UK, Milton Keynes, UK). In some cases a 'minislice' was prepared, in which the MSDB was dissected away from surrounding structures with a small scalpel. For extracellular and sharp electrode recordings, the slices were transferred to an interface recording chamber where they were routinely maintained at a temperature of 33°C, at the interface between warm humidified carbogen gas (95% O_2–5% CO_2) and ACSF containing (mM): 126 NaCl, 3 KCl, 1.25 NaH_2PO_4, 24 $NaHCO_3$, 2 $MgSO_4$, 2 $CaCl_2$, 10 glucose (Fisahn *et al.* 1998). The slices were allowed to equilibrate for 1 h prior to recording.

Where specifically mentioned in the text, experiments were also performed at 37°C. At temperatures of both 33°C and 37°C, it was essential to maintain the temperature and oxygenation of the slices and to preserve a high level of humidity within the environment of the recording chamber to prevent the slices from drying out. To ensure these conditions were met, the recording chamber was kept covered at all times with two microscope slices. From time to time, condensation was wiped off from underneath the slides to prevent contamination of the slices with water of condensation. During recording sessions, a 3–4 mm gap was allowed between the microscope slices to accommodate up to two recording electrodes. Temperature was routinely and continuously monitored using a temperature probe placed in the oxygenated and heated water reservoir underneath the recording chamber; ACSF passes through this reservoir in coiled plastic tubing before it encounters the slice in the recording chamber. To check beforehand that the temperature regulation of the slice was adequate when recordings were being carried out, the temperature of the ACSF next to the slice was measured as well as that within the reservoir by using two temperature probes. Provided that the recording chamber was kept covered with the microscope slides, a difference of only 0.3°C was noted between the ACSF next to the slice and the water in the heated reservoir. For recordings performed at 37°C, therefore, the temperature of the reservoir was routinely set at 37 ± 0.3°C.

Recording, data acquisition and analysis

For the recordings, one or both channels of an Axoprobe 1A amplifier (Axon Instruments, Union City, CA, USA) were employed, one for extracellular recording and the other for intracellular recording, or both for dual extracellular recording. Extracellular field recordings were made using glass microelectrodes containing ACSF (resistance 2–5 MΩ). Intracellular recordings were made with glass microelectrodes containing 2 M potassium acetate (pH 7.4, electrode resistance 80–150 MΩ). In some cases 2% biocytin (Sigma, Poole, Dorset, UK), or 50 mM QX-314 (lidocaine *N*-ethyl bromide, $C_{16}H_{27}BrN_2O$, Tocris

Cookson Ltd, Bristol, UK) was included with the intracellular electrode solution. Intracellular recordings were made in the conventional current clamp mode, and bridge balance was monitored using small hyperpolarizing current pulses (50 pA; 100 ms duration). Data were band-pass filtered online between 0.5 Hz and 0.5–2 kHz using the Axoprobe amplifier or a Neurolog system NL106 AC/DC amplifier (Digitimer Ltd, Welwyn Garden City, UK). The data were digitized at a sample rate of 5–10 kHz using an ITC-16 ADC board (Digitimer Ltd). Mains frequency interference was eliminated from extracellular recordings with the use of a 50 Hz noise eliminator (HumBug; Digitimer Ltd). For intracellular recordings from neurones, the presence of time-dependent inward rectification (depolarizing sag), and the properties of single action potentials and firing patterns of the neurones, were determined as previously described for the MSDB (Morris *et al.* 1999; Morris & Henderson, 2000; Knapp *et al.* 2000; Henderson *et al.* 2001).

Data were further analysed off-line using software from Axograph (Axon Instruments), KaleidaGraph (Synergy Software, Reading, PA, USA) and SigmaStat (SPSS Inc., CA, USA). Power spectra were used to provide a quantitative measure of the frequency components in a stretch of recording, where power, a quantitative measure of the oscillation strength, was plotted against the respective frequency. Power spectra were constructed for 60 s epochs of extracellular field recordings using a fast Fourier transform algorithm provided by the Axograph software. The parameters used for measuring the oscillatory activity in the slice were: (1) peak frequency (Hz), (2) power at peak frequency ($\mu V^2\ Hz^{-1}$) and area power (μV^2). In the current study (unless indicated otherwise), area power was equivalent to the computed area under the power spectrum between the frequencies of 4 and 15 Hz. Autocorrelation analyses were carried out to provide a qualitative measure of the rhythmicity of the activity, in which the autocorrelation function gives a measure of how a signal is correlated with itself over different time lags. Action potential activity recorded with intracellular electrodes was analysed by the construction of interspike interval histograms. The relationships between the action potential firing of a single cell and the phase or distance in time from the peak or trough of the network oscillation were also shown as histograms. Results were expressed as mean ± standard deviation (unless indicated otherwise), and statistical significance was determined with Student's *t* test, the Mann-Whitney rank sum test, or ANOVA, with significance levels of $P < 0.05$.

Anatomical identification of MSDB neurones

Anatomical studies were performed on the slices (1) to determine whether oscillatory activity recorded with the extracellular field electrode was localized within areas of the MSDB that contained parvalbumin-containing neurones, and (2) for neurochemical characterization of cells that had been recorded from intracellularly and filled with biocytin. After extracellular recording, the position of the extracellular recording electrode was marked by driving the tip of the electrode deep into the slice so that it produced a visible electrode track in the fixed tissue. If multiple extracellular recordings were being made from the slice, the positions of the electrodes relative to visible landmarks were marked on a diagram of the slice as the experiment was being carried out. After intracellular recording, the cells were filled with biocytin using hyperpolarizing current pulses (500 ms, 1 Hz, 0.2–0.3 nA) for 15–60 min. Slices were then placed gently between two pieces of filter paper (Millipore UK Ltd), and fixed overnight in 4% paraformaldehyde at 4°C. The slices were then washed several times in 0.1 M phosphate buffer (pH 7.4), embedded in gelatin and sectioned at 50–75 μm using a Leica VT1000S vibrating microtome.

To establish the positions of the field electrodes with respect to the distribution of parvalbumin-containing neurones, the sections were stained for parvalbumin immunoreactivity using an immunofluorescence technique. The sections were incubated for 1–2 days at 4°C, in 1 : 3000 mouse anti-parvalbumin (PARV-19, Sigma) and 1 : 3000 of a second mouse anti-parvalbumin antibody (PA-235, Sigma), with 2% bovine serum albumin, 0.1% Triton and 0.02% sodium azide in phosphate-buffered saline (PBS, pH 7.4). The sections were then washed several times in 'wash' solution consisting of 0.1% Triton in PBS, which was also the vehicle for the secondary antibody solutions. The sections were then incubated for 2 h in the dark at room temperature in 1 : 1000 goat anti-mouse IgG conjugated to CY3 (Stratech Scientific Ltd, Soham, UK). The sections were washed several times and mounted in Vectamount (Vector Laboratories, Peterborough, UK), and viewed with a fluorescence microscope.

To determine the neurochemical identities of the neurones that had been recorded from using sharp electrodes and filled with biocytin, the sections were incubated in 1 : 1000 streptavidin–Alexa 488 (Molecular Probes Europe BV, Leiden, The Netherlands) for 2–3 h in the dark at room temperature to visualize the biocytin. The sections were washed several times, and processed for parvalbumin immunoreactivity as described above, then mounted on slides in VectaShield mounting medium.

Additional data to support the results were obtained from immunocytochemical staining and Neurolucida (MicroBrightField Europe, Magdeburg, Germany) mapping procedures carried out on perfused-fixed tissue obtained from three adult rats (200 g). The rats were deeply anaesthetized with an intraperitoneal injection of ketamine (140 mg kg^{-1}, Fort Dodge Animal Health Ltd,

Southampton, UK) and xylazine (14 mg kg^{-1}, Millpledge Pharmaceuticals, UK). The rats were perfused intracardially with 500 ml of 4% paraformaldehyde in 0.1 M phosphate buffer. The brains were removed and placed in the same fixative for 2–3 h, and then in phosphate buffer overnight at 4°C. Sections were cut at 50 μm using a Leica VT1000S microtome and processed for immunocytochemistry. All steps were carried out at room temperature and in 0.1% Triton in PBS unless mentioned otherwise. The sections were incubated for 1 h in 2% bovine serum albumin, and then alternate sections, kept in serial order, were incubated overnight at 4°C in 1 : 4000 goat anti-vesicular acetylcholine transporter (VAChT; Chemicon International Inc., Harrow, UK) or 1 : 3000 mouse anti-parvalbumin (PARV-19 Sigma); VAChT immunoreactivity is a marker for cholinergic neurones. Both antibody solutions were made up in 2% bovine serum albumin, 0.1% Triton and 0.02% sodium azide in PBS (pH 7.4). The sections were then washed several times and incubated for 2 h with 1 : 1000 biotinylated horse anti-goat or anti-mouse IgG (Vector Laboratories), respectively. Following several washes, the sections were

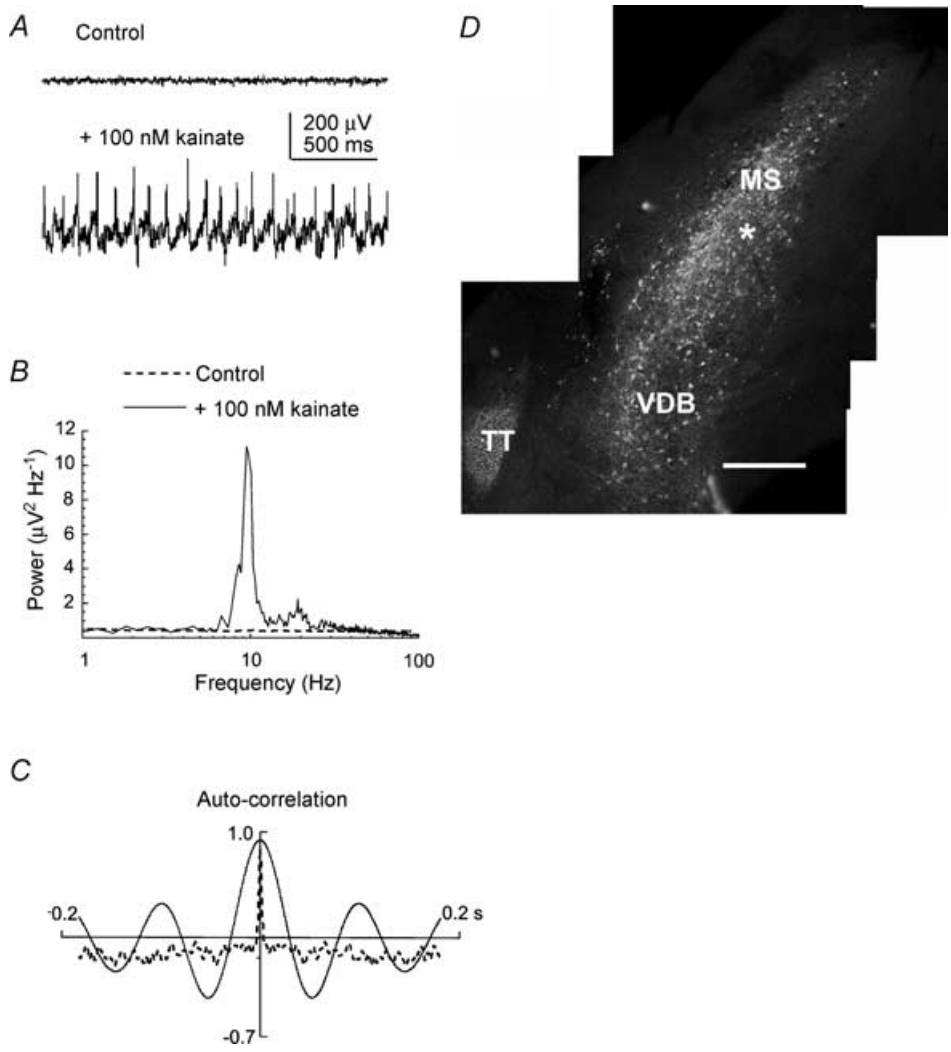

Figure 1. Characterization of theta frequency oscillatory activity in the parasagittal slice of the medial septum–diagonal band (MSDB) complex

A, example extracellular field recordings from the surface of the MSDB parasagittal slice before (above) and during (below) bath application of 100 nM kainate. *B*, example power spectrum of a recording of rhythmic extracellular field activity exhibiting a prominent peak in the theta frequency range (4–15 Hz). *C*, the corresponding autocorrelograms show that the extracellular field activity following application of the kainate (continuous line) was rhythmic. *D*, distribution of parvalbumin immunofluorescence in a section from an MSDB slice in which the recording site of the extracellular electrode was marked (asterisk) by driving the electrode into the tissue after the recording was made. Calibration bar, 400 μm. MS, medial septum; VDB, vertical nucleus of the diagonal band; TT, taenia tecta (a cortical-derived structure that stains positively for parvalbumin immunoreactivity).

Table 1. Characteristics of kainate-induced theta frequency oscillations in the MSDB slice recorded over a 4 and 8 h period

	Peak frequency (Hz)	Power at peak frequency (μV^2 Hz^{-1})	Area power (μV^2)
Baseline activity ($n = 8$)	9.5 ± 4.3	6.2 (3.5–17.9)	31.5 (19.5–64.5)
Activity after 4 h in kainate ($n = 8$)	9.8 ± 4.4	9.2 (3.3–19.0)	30.8 (17.8–61.2)
Baseline activity ($n = 4$)	10.8 ± 4.8	15.2 (3.6–22.9)	35.8 (20.5–73.7)
Activity after 8 h in kainate ($n = 4$)	9.7 ± 3.0	13.3 (3.1–27.3)	35.3 (21.1–65.4)

Values are mean ± S.D. in column 2, and mean and interquartile range (in parentheses) in columns 3 and 4.

incubated for 2 h in 1 : 25 avidin–biotin horseradish peroxidase complex. The sections were then washed in 0.1 M phosphate buffer followed by 0.05 M Tris buffer at pH 8.0, and then incubated for 5–10 min in 0.006% H_2O_2, 0.014% diaminobenzidine and 0.6% nickel ammonium sulphate in 0.05 M Tris buffer at pH 8.0. This reaction produced an intense black precipitate as staining for VAChT or parvalbumin immunoreactivity (Wouterlood *et al.* 1987). The sections were then mounted on slides under coverslips in solvent-based mounting medium in the conventional manner. The distribution of the stained neurones in midline parasagittal sections of the MSDB were mapped using a × 100 oil objective and a microscope equipped with the Neurolucida neurone mapping package.

Materials

All standard reagents, except where indicated, were obtained either from Sigma (UK) or VWR International (Lutterworth, UK). 2*S*,3*S*,4*R*-Carboxy-4-(1-methylethenyl)-3-pyrrolidineacetic acid (kainate, or kainic acid), bicuculline methochloride, GABAzine, 2,3,-dioxo-6-nitro-1,2,3,4-tetrahydrobenzo[f]quinoxaline-7-sulphonamide disodium (NBQX), baclofen, CGP55845, D(−)-2-amino-5-phosphonopentanoic acid (D-AP5) and SYM 2206, were purchased from Tocris Cookson Ltd (Bristol, UK). 1-Octanol, atropine sulphate, biocytin HCl, carbenoxolone, diazepam and mecamylamine (MCA) were obtained from Sigma (UK). Stock solutions, at × 1000 working concentrations, were made up in water, except for NBQX and CPG55845 which were made up in DMSO and stored in individual aliquots at −45°C.

Results

General features of the oscillations obtained with bath-applied kainate to the MSDB *in vitro*

To study the induction of network oscillations in the MSDB slices, we used bath application of nanomolar concentrations of kainate, a pharmacological protocol previously used to induce synchronized oscillatory activity in slices of hippocampus and entorhinal cortex (Traub *et al.* 2000; Hormuzdi *et al.* 2001; Cunningham *et al.* 2003). The bath application of kainate at doses of 50–300 nM, the operational range used for eliciting oscillatory activity in cortical areas (e.g. Cunningham *et al.* 2003), evoked oscillatory field activity that was recordable from the surface of the longitudinal MSDB slice. This oscillatory activity became evident at about 20 min after bath application of the kainate and was well established by 1 h afterwards. The oscillatory activity was evident from inspection of the raw trace (e.g. Fig. 1*A*), from the peak in the power spectrum (e.g. Fig. 1*B*) and from the sinusoidal mode of the autocorrelogram (e.g. Fig. 1*C*). There was no evidence for a peak in the power spectrum when the slice was 'at rest', but in this condition the area power (between 4 and 15 Hz) was never zero, due to baseline non-oscillatory electrical activity and/or intrinsic noise (e.g. Fig. 1*A* and *B*). Thus in a set of preliminary experiments ($n = 50$), the presence of kainate produced a significant increase in area power of the power spectrum ($P < 0.001$; Mann-Whitney rank sum test), with peak frequency occurring at 8.3 ± 3.7 Hz (range 4–16 Hz), power at peak frequency at 9.2 ± 40.6 μV^2 Hz^{-1}, and area power at 38.6 ± 20.0 μV^2. The effect of the bath-applied kainate was reversible: the power at peak frequency was significantly reduced by 65.6 ± 11.6% 1 h after washout of the bath-applied kainate ($P < 0.05$; paired *t* test; $n = 4$). Without washout, the kainate-induced oscillatory activity in the MSDB slice persisted from 4 h ($n = 8$) to 8 h ($n = 4$), without significant change in peak frequency, power at peak frequency or area power (ANOVA; $P < 0.05$; Table 1). Extracellular theta frequency activity was also successfully recorded from coronal slices of the MSDB exposed to 50–300 nM kainate, with peak frequency occurring at 6.4 ± 1.3 Hz, power at peak frequency at 11.4 ± 4.4 μV^2 Hz^{-1}, and area power at 40.4 ± 39.2 μV^2 ($n = 7$).

For consistency, all subsequent experiments described (except for those carried out at 37°C; see below), were conducted with 100 nM kainate, the lowest concentration at which oscillatory activity was reliably

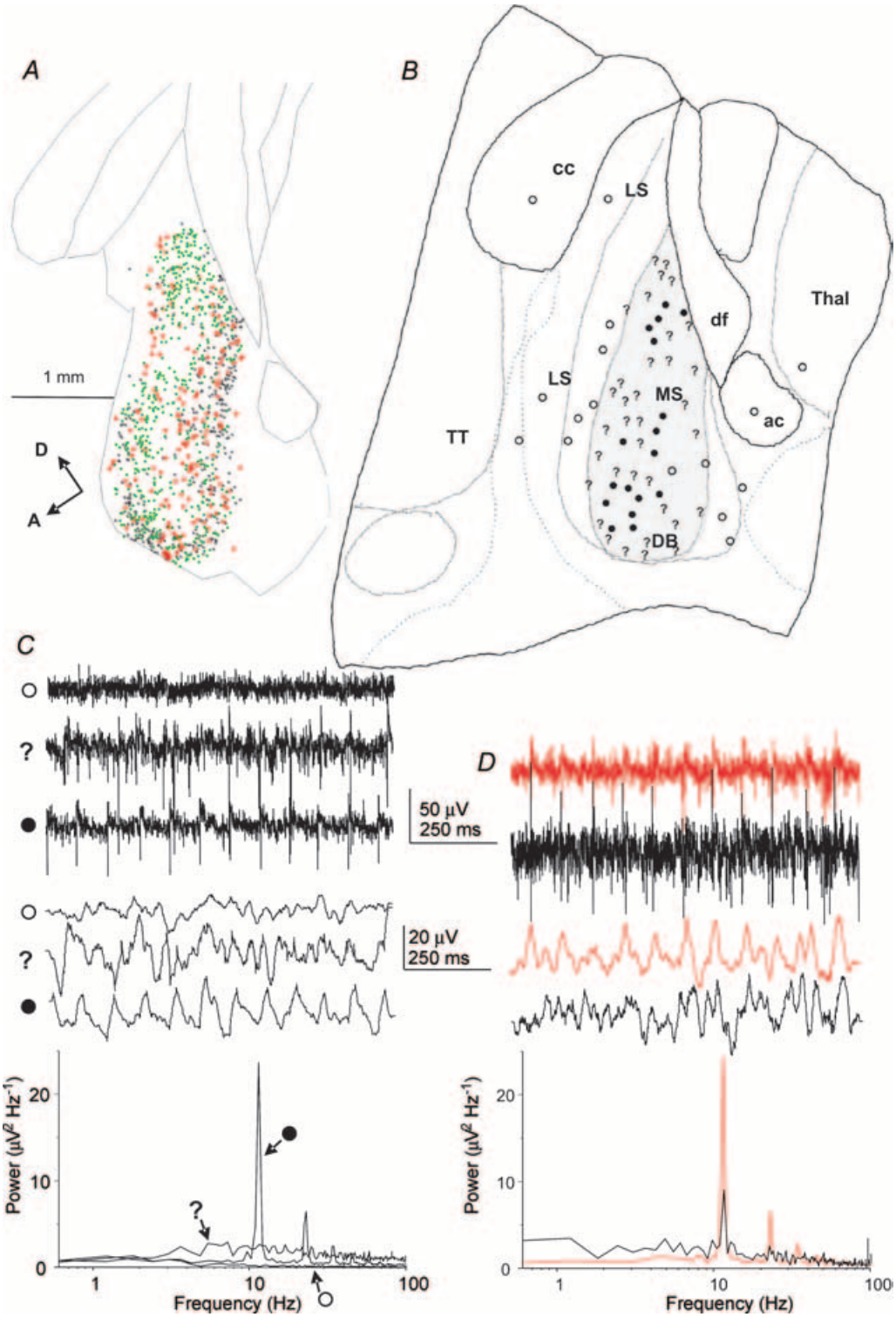

Figure 2. Location of theta frequency field activity, in conjunction with the distribution of different neurone cell types within the parasagittal slice of the MSDB

A, distribution of the VAChT-immunoreactive neurone and two types of parvalbumin-immunoreactive neurone (Henderson *et al.* 2004) in a longitudinally cut, 50 μm section from the midline MSDB of adult, perfused-fixed rat brain. The cells were mapped using the Neurolucida system, and individual VAChT-positive neurones are indicated by black stars. Parvalbumin-positive neurones surrounded by parvalbumin-positive boutons are indicated by green squares, and parvalbumin-positive neurones that lack such boutons are indicated by red circles. Calibration bar, 1 mm. A, anterior; D, dorsal. *B*, diagram of a slice (drawn with the aid of a camera lucida attachment), corresponding to the region represented by the section in *A*, showing the distribution of three types of extracellular field activity

recorded, and with longitudinally cut slices. To confirm that neighbouring structures in the slice were not contributing to the kainate-induced generation of theta frequency oscillations in the MSDB, a number of longitudinal slices were prepared in which all structures surrounding the MSDB were carefully removed using a small scalpel knife ($n = 4$). The parameters of the activity recorded from these preparations following the application of 100 nM kainate (peak frequency 13.9 ± 3.2 Hz; area power 17.7 ± 0.5 μV^2) were comparable to those recorded from the regular slices. In order to eliminate the possibility of damage caused to the structure by dissection, and to maintain consistency, the working MSDB slice was routinely prepared with its surrounding structures intact (e.g. as illustrated in Fig. 2*B*).

Topographical distribution of the kainate-induced oscillatory activity

Post hoc staining of slices for parvalbumin immunoreactivity indicated that the sites from which oscillatory theta activity could be recorded were within areas containing parvalbumin-immunoreactive neurones ($n = 6$; see example in Fig. 1*D*). In a further five experiments, the topography of the kainate-induced oscillatory activity in the MSDB slice was examined by recording from numerous sites in the MSDB and surround using two roving extracellular electrodes. Three types of activity were scored: (1) no activity, in which the baseline recording was flat and had no peak in the power spectrum (e.g. as indicated by the open circles in Fig. 2*B* and *C*); (2) disorganized activity, where there was a visible increase in the amplitude of the activity in the raw and digitally filtered traces, but no discernable peak in the power spectrum (e.g. as indicated by a question mark symbol in Fig. 2*B* and *C*); and (3) rhythmic activity visible in the raw and digitally filtered traces, and which had a discernable peak in the power spectrum (e.g. as indicated by the filled circles in Fig. 2*B* and *C*). In all five experiments the oscillatory activity was confined almost exclusively to the midline slice and virtually no rhythmic activity was found in the two slices on either side of it. In these experiments both the rhythmic and the 'disorganized' activities were confined to the areas of the MSDB that contained parvalbumin-immunoreactive somata (e.g. Fig. 2*A* and *B*). No conclusions could be drawn from these experiments, however, about whether the rhythmic activity was being recorded from dendrites or somata, or both, as the MSDB is not layered like the hippocampus. Whilst the distribution of labelling shown in Fig. 2*A* indicates the positions of individual immunoreactive somata, some MSDB neurones have been shown to have dendrites that extend over the breadth of the MSDB in the anterior–posterior direction (Henderson *et al.* 2001). The localization procedure described here is therefore essentially coarse-grained. When recordings were performed simultaneously with two electrodes placed in different parts of the MSDB, no coherence was observed in the rhythmic activity unless the two electrodes were less than 200 μm apart ($n = 5$, e.g. Fig. 2*D*). Mean peak frequencies of the rhythmic activity for each of the five experiments were 11.5 ± 2.2 Hz ($n = 6$); 8.8 ± 2.7 Hz ($n = 6$), 10.1 ± 3.2 Hz ($n = 13$), 8.4 ± 2.7 Hz ($n = 19$) and 11.9 ± 2.5 Hz ($n = 7$).

Effects of neurotransmitter receptor antagonists on kainate-induced oscillatory activity

In any network producing synchronous rhythmic activity, the interplay between interconnecting cell types and afferent input is paramount. Therefore the putative roles of glutamatergic, GABAergic and cholinergic receptors in generating this model of theta activity were investigated by application of receptor antagonists. Because it was not possible to predict exactly where the rhythmic activity would be before the application of kainate, in most experiments the rhythmic activity was localized after the addition of kainate and then the effect of adding the antagonist was assessed. Extracellular theta frequency oscillations were evoked in the MSDB slices by bath application of 100 nM kainate and were allowed 60 min to stabilize before the application of the antagonist agent. Extracellular field activity was recorded at 10, 20, 30 and 60 min after addition of the antagonist, and if there was any change, the slice was then superfused for up to an hour with 100 nM kainate without the antagonist to assess the degree of recovery of the extracellular activity. Results in the figures are presented at 60 min after application of

recorded in the presence of 100 nM kainate: o, no activity; ?, disorganized activity; and ●, rhythmic activity; examples of the activity are illustrated in *C*. The grey-shaded area is where parvalbumin-positive neurones were found to be distributed after staining the slice *post hoc* for parvalbumin immunoreactivity. cc, corpus callosum; LS, lateral septum; , MS, medial septum; DB diagonal band; ac, anterior commissure; Thal, thalamus; TT, taenia tecta. *C*, three different types of extracellular field activity are shown, which correspond to the symbols used to map these activities in *B*. Top, raw traces; middle, traces digitally filtered using the Axograph 'box car' program (100 points); bottom, power spectra computed from 30 s traces. *D*, example recordings (corresponding in format to those shown in *C*) of activity recorded from two electrodes 100 μm apart, showing some measure of coherence in the oscillatory field activity.

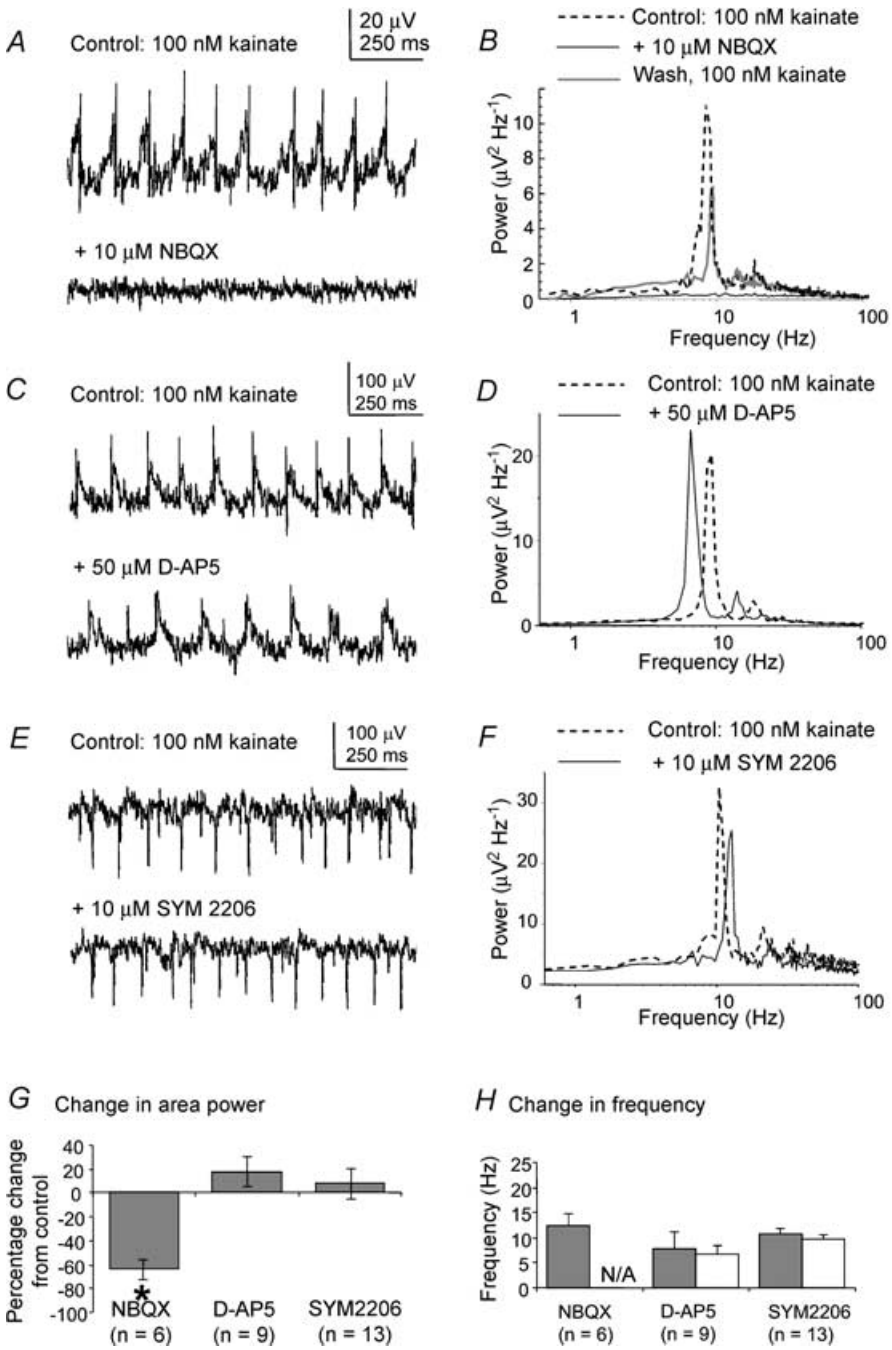

Figure 3. Effects of glutamate receptor antagonists on kainate-induced oscillatory activity in the MSDB slice

A, example traces of extracellular oscillatory activity recorded in MSDB slices in the presence of 100 nM kainate, before and after the application of 10 μM NBQX, a glutamate receptor antagonist specific for AMPA and kainate receptors. *B*, corresponding power spectra showing that NBQX abolishes the theta peak in the power spectrum, with recovery of the peak after removal of the antagonist. *C*, example traces of extracellular oscillatory activity recorded in MSDB slices in the presence of 100 nM kainate, before and after the application of 50 μM D-AP5, a glutamate receptor antagonist specific for NMDA receptors. *B*, corresponding power spectra showing that D-AP5 had minimal effect on the theta peak in the power spectrum. *E* and *F*, traces analogous to those above, but for 10 μM SYM 2206, a glutamate receptor antagonist specific for AMPA receptors, showing minimal effect on the theta peak in the power spectrum. *G*, group data showing the percentage change in area power of activity for all the receptor antagonists tested. Asterisk indicates statistical significance ($P < 0.05$). The error bars represent standard errors of the mean (S.E.M.). *H*, group data showing the change in frequency of the rhythmic activity for all the receptor antagonists tested. N/A indicates there was no discernable peak in the power spectrum after addition of the antagonist. The error bars represent standard deviations (S.D.).

Table 2. Changes in area power (μV^2) of the kainate-induced oscillatory activity, 60 min after the application of various antagonists and modulators of neural transmission

Antagonist	Area power in the presence of 100 nM kainate at 0 min	Area power in the presence of 100 nM kainate 60 min after application of the antagonist	Recovery after 60 min in the presence of 100 nM kainate alone
NBQX ($n = 6$)	55.4 ± 41.2	17.2 ± 9.4*	39.5 ± 34.1
D-AP5 ($n = 9$)	26.3 ± 17.1	30.4 ± 23.0	—
SYM 2206 ($n = 13$)	84.5 ± 110.8	61.0 ± 39.6	—
Bicuculline ($n = 7$)	64 ± 88.2	36.3 ± 40.2*	56.7 ± 77.2
CGP55845 ($n = 4$)	23.6 ± 20.8	24.9 ± 20.6	—
Diazepam ($n = 4$)	2.9 ± 0.7	3.1 ± 0.9	—
Atropine ($n = 6$)	8.7 ± 3.2	9.9 ± 3.4	—
Mecamylamine ($n = 3$)	77.9 ± 15.5	77.2 ± 14.1	—
Carbenoxolone ($n = 5$)	21.3 ± 13.7	4.4 ± 3.9	—
Octanol ($n = 3$)	10.8 ± 8.5	3.3 ± 2.9	—

Values are mean ± S.D. *Statistically significant change ($P < 0.05$) from the previous value (see text for details of the statistical tests used).

the pharmacological agents, even if changes had occurred more rapidly than this.

We first examined the effects of ionotropic glutamate receptor antagonists on the rhythmic activity induced by kainate in the MSDB. The area power of the kainate-induced oscillatory activity in the MSDB slice was significantly reduced from 55.4 ± 41.2 to $17.2 \pm 9.4\ \mu V^2$ following bath application of 10 μM of the AMPA/kainate receptor antagonist NBQX ($P < 0.05$; ANOVA with Tukey's test; $n = 6$), with recovery of area power to $39.5 \pm 34.1\ \mu V^2$ after removal of the antagonist (e.g. Fig. 3*A* and *B*, and *G* and *H* for group data). The peak of the power spectrum was virtually eliminated during the application of NBQX (e.g. Fig. 3*A* and *B*). There was no significant change in area power or of peak frequency of the kainate-evoked theta frequency field potential following bath application of 50 μM of the NMDA receptor antagonist D-AP5 ($P > 0.05$, paired *t* test, $n = 9$, e.g. Fig. 3*C* and *D*, and *G* and *H* for group data). There was also no significant change either in area power ($P > 0.05$, Wilcoxon test, $n = 13$) or of peak frequency ($P > 0.05$, paired *t* test, $n = 13$) of the kainate-evoked theta frequency field potential following the bath application of 10 μM of the AMPA receptor antagonist SYM 2206 (e.g. Fig. 3*E* and *F*, and *G* and *H* for group data). The absolute values for area power are summarized in Table 2.

We next looked at the effects of antagonists and modulators of GABA receptor transmission on kainate-induced rhythmic activity in the MSDB slice. There was a significant reduction in area power of the kainate-induced, theta frequency field activity, from 64 ± 88.2 to $36.3 \pm 40.2\ \mu V^2$, following the bath application of 10 μM of the $GABA_A$ receptor antagonist bicuculline, with no major peak activity remaining in the power spectrum ($P < 0.05$, Wilcoxon test, $n = 7$, e.g. Fig. 4*A* and *B*, and *G* and *H* for group data). There was recovery after removal of the bicuculline from the recording chamber, with the area power increasing from 36.3 ± 40.2 to $56.7 \pm 77.2\ \mu V^2$, and there was a return of a theta peak in the power spectrum (Fig. 4*B*). Bath application of 1 μM of the $GABA_B$ receptor antagonist CGP55845 had no significant effect on the peak frequency or area power of the oscillatory activity ($P > 0.05$, paired *t* test; $n = 4$, e.g. Fig. 4*C* and *D*, and *G* and *H* for group data).

To determine whether $GABA_A$ receptor IPSPs might have a role in the oscillatory process in the MSDB, the effect of IPSP modulation was examined. Experimentally, the time course of IPSPs can be slowed by benzodiazepines, and application of diazepam to hippocampal slices during gamma frequency activity produces a concentration-dependent decrease in the frequency of the oscillatory activity (Traub *et al.* 1996). To determine whether similar mechanisms underlie the generation of theta frequency activity in the MSDB model, 10 μM diazepam was bath-applied to stabilized kainate-evoked theta oscillations in the MSDB slice. The result was a significant reduction in the peak frequency of the activity induced by kainate, from 12.3 ± 1.3 to 9.7 ± 1.0 Hz by 30 min, and to 6.4 ± 0.6 Hz after 60 min ($P < 0.05$, paired *t* test, $n = 4$). There was no significant effect on area power ($P > 0.05$, *t* test, $n = 4$, e.g. Fig. 4*E* and *F*, and *G* and *H* for group data). The results of these experiments on area power are summarized in Table 2.

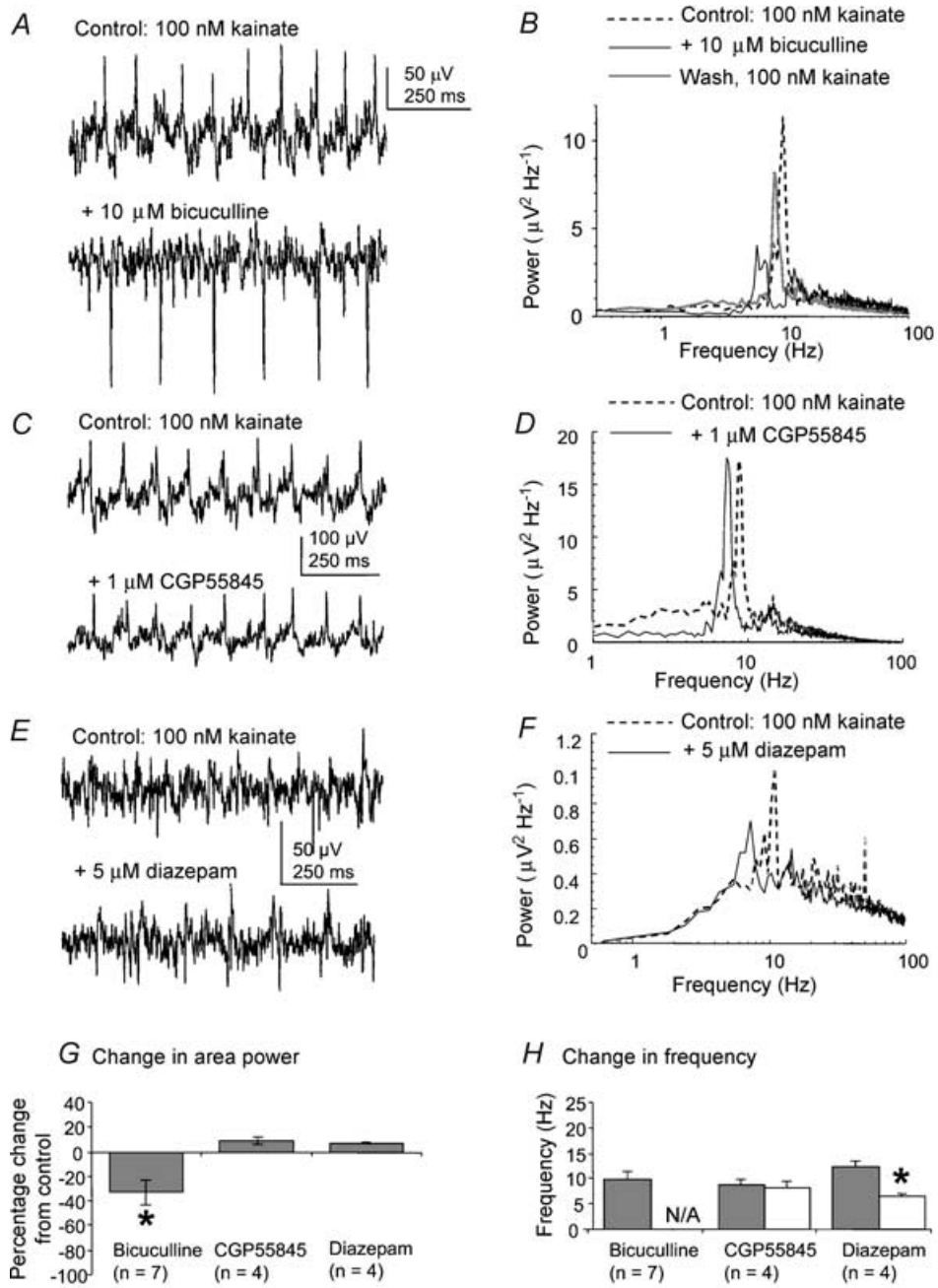

Figure 4. Effects of GABA receptor antagonists and modulators on kainate-induced oscillatory activity in the MSDB slice

A, example traces of extracellular oscillatory activity recorded in MSDB slices in the presence of 100 nM kainate, before and after the application of 10 μM bicuculline, a GABA receptor antagonist specific for $GABA_A$ receptors. *B*, corresponding power spectra showing that bicuculline reduces the theta peak in the power spectrum, with recovery after removal of the antagonist. *C*, example traces of extracellular oscillatory activity recorded in MSDB slices in the presence of 100 nM kainate, before and after the application of 1 μM CGP55845, a GABA receptor antagonist specific for $GABA_B$ receptors. *D*, corresponding power spectra showing that CGP55845 had minimal effect on the theta peak in the power spectrum. *E*, example traces of extracellular oscillatory activity recorded in MSDB slices in the presence of 100 nM kainate, before and after the application of 5 μM diazepam, a drug that slows the kinetics of $GABA_A$ receptor IPSPs. *F*, corresponding power spectra showing that diazepam reduces the peak frequency of the power spectrum. *G*, group data showing the percentage change in area power of activity for all the receptor antagonists tested. Asterisk indicates statistical significance ($P < 0.05$). The error bars represent S.E.M. *H*, group data showing the change in frequency of the rhythmic activity for all the receptor antagonists tested. N/A indicates there was no discernable peak in the power spectrum after addition of the antagonist. Asterisk indicates statistical significance ($P < 0.05$). The error bars indicate S.D.

Finally, we examined the role of cholinergic receptors in the kainate-induced activity in the MSDB slice. Bath application of 2–10 μM of the muscarinic receptor antagonist atropine sulphate had no significant effect on the area power (Table 2) or frequency of the kainate-induced oscillations in the MSDB ($P > 0.05$, paired t test, $n = 6$, see Fig. 5*C* for group data). Bath application of 25–50 μM of the nicotinic receptor antagonist mecamylamine similarly had no significant effect on area power (Table 2) or frequency of the oscillatory activity ($P > 0.05$, paired t test, $n = 3$, see Fig. 5*C* for group data). Concomitant blockade of both types of cholinergic receptors, on the other hand, resulted in a change in both the area power and peak frequency of the oscillation recorded. Bath application of a combination of the two antagonists mecamylamine (25 μM) and atropine sulphate (2 μM), resulted in a significant shift in the main frequency peak from 8.1 ± 2.5 to 16.2 ± 4.6 Hz ($P < 0.001$, paired t test, $n = 10$, Fig. 5*A* and *B*, and *C* for group data). This was accompanied by a significant increase in the power of the oscillatory activity of the slice within the 15–30 Hz frequency band from 50.1 ± 95.6 to 59.4 ± 92.4 μV^2 ($P < 0.05$, paired t test, $n = 10$). Upon washout of the antagonist, this peak frequency shift was returned to within the theta band range at 10.4 ± 1.6 Hz (Fig. 5*A* and *B*). In 4 out of 10 experiments, a second prominent peak of activity at 6.9 ± 2.3 Hz remained in the theta band following combined application of the cholinergic receptor antagonists (not illustrated). The results for area power are summarized in Table 2.

Effects of putative gap junction blockers

Recently it has been shown that gap junctions play a role in the generation of gamma frequency oscillatory activity in the hippocampus slice (Hormuzdi *et al.* 2001; Traub *et al.* 2004) and theta frequency oscillatory activity in the thalamus slice (Hughes *et al.* 2004). The possible role of electrotonic coupling on the kainate-induced theta activity in the MSDB slice was therefore examined by the application of two putative gap junction blockers octanol and carbenoxolone, which have been shown to block pharmacologically evoked oscillations in slices of the hippocampus (Traub *et al.* 2000; LeBeau *et al.* 2002) and thalamus (Hughes *et al.* 2004). Bath application of 100 μM carbenoxolone resulted in a reduction of the area power of the oscillations from 21.3 ± 13.7 to 4.4 ± 3.9 μV^2 with no remaining peak (e.g. Fig. 5*D* and *E*, and *H* for group data). Similarly, application of 1–2 mM octanol produced a reduction in the area power from 10.8 ± 8.5 to 3.3 ± 2.9 μV^2, with no remaining peak activity (e.g. Fig. 5*F* and *G*, and *H* for group data). The results for area power are summarized in Table 2.

Recordings at 37°C and with different doses of kainate

Additional experiments were performed to determine whether the average frequency and frequency range of kainate-induced oscillations are maintained within the theta range at temperatures of 37°C, and with concentrations of kainate ranging from 50 to 300 nM. In the first group of experiments ($n = 7$ slices; $n = 12$ recording sites) the slices were superfused with 100 nM kainate at 37°C. The mean frequency of the oscillatory activity in these experiments was 9.1 ± 2.4 Hz (range 6.7–14.0 Hz), with peak power at 9.1 ± 10.1 μV^2 Hz^{-1} and area power at 37.2 ± 30.3 μV^2.

A second group of experiments was then carried out ($n = 5$ slices, $n = 7$ recording sites) where increasingly higher doses of kainate (50–300 nM) were added to the MSDB slice maintained at 37°C. To confirm that the oscillatory activity observed under these conditions was due to network activity, 0.25 μM baclofen, a $GABA_B$ receptor agonist, was then added, followed by CGP55845, a $GABA_B$ receptor antagonist ($n = 7$). Previously we have shown that doses of baclofen lower than 1 μM depress synaptic activity via presynaptic $GABA_B$ receptors in the MSDB slice, without having any discernable effect on postsynaptic $GABA_B$ receptors (Henderson & Jones, 2005). In some cases 20 μM GABAzine, a $GABA_A$ receptor antagonist, was added at the end of the experiment ($n = 4$). Recordings were taken every 5–10 min, and each reagent was added after stabilization of any change in frequency and area power that may have occurred after application of the previous reagent, usually by 30–40 min. In five out of seven cases, the addition of increasing doses of kainate from 50 nM to 300 nM caused a systematic rise in the area power and frequency of the oscillatory activity, but the frequency of the oscillatory activity remained within the theta range (see example in Fig. 6*A* and *B*, and see Fig. 6*C* and *D* for group data and significance levels). The further addition of 0.25 μM baclofen significantly reduced the frequency of the oscillatory activity from 11.5 ± 2.5 to 7.7 ± 0.9 Hz, and the frequency was restored to 11.2 ± 2.0 Hz by the application of 1 μM CGP55845 ($P < 0.05$, ANOVA with Tukey's test, $n = 5$, Fig. 6*A*, *B* and *D*). There was also a decrease in area power upon the addition of baclofen, and restoration of the area power after the addition of the CGP55845, but these effects were not statistically significant ($P > 0.05$, ANOVA with Tukey's test, $n = 5$, Fig. 6*C*). The theta frequency peak in the oscillatory activity was either substantially reduced or abolished by the addition of 20 μM GABAzine ($n = 3$; Fig. 6*A*, *B* and *D*). The area power was also reduced by GABAzine, but not significantly ($n = 3$; Fig. 6*C*). In 2 out of 7 experiments the frequency of the oscillatory activity in the presence of increasing doses of kainate increased to values above 20 Hz, but the frequency or area power of this

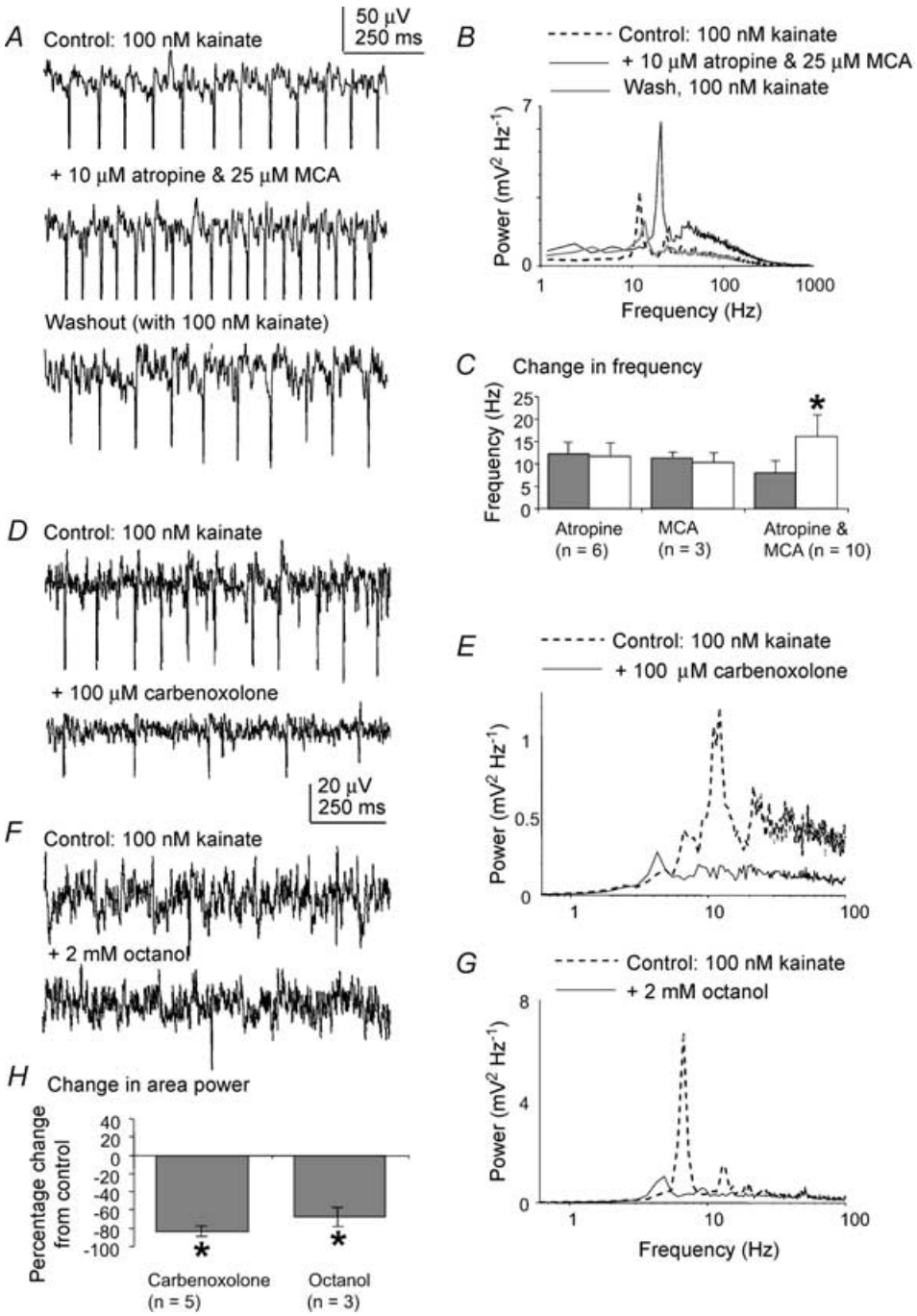

Figure 5. Effects of cholinergic receptor and putative gap junction antagonists on kainate-induced oscillatory activity in the MSDB slice

A, example traces of extracellular oscillatory activity recorded in MSDB slices in the presence of 100 nM kainate, before and after the application of a combination of 10 μM atropine and 25 μM mecamylamine (MCA), cholinergic receptor antagonists specific for muscarinic and nicotinic receptors, respectively, and after washout of the antagonists with 100 nM kainate. *B*, corresponding power spectra showing that concomitant blockade of muscarinic and nicotinic receptors increases the peak frequency of the oscillatory activity, with the peak reverting to theta frequencies after removal of the antagonists. *C*, group data showing the change in frequency of the activity for all the combinations of cholinergic receptor antagonists tested. Asterisk indicates statistical significance ($P < 0.05$) and the error bars indicate S.D. *D*, example traces of extracellular oscillatory activity recorded in MSDB slices in the presence of 100 nM kainate, before and after the application of 100 μM carbenoxolone, a gap junctional blocker. *E*, corresponding power spectra showing that carbenoxolone abolishes the theta peak in the power spectrum. *F*, example traces of extracellular oscillatory activity recorded in MSDB slices in the presence of 100 nM kainate, before and after the application of 2 mM octanol, a gap junctional blocker. *G*, corresponding power spectra showing

activity did not change upon the addition of baclofen or GABAzine. This suggested that the oscillatory activity that was being recorded in these two latter cases was not based on intact synaptic connectivity.

Firing activity of cell types in the MSDB during kainate-induced theta frequency activity in the MSDB slice

To investigate the patterns of firing activity of different MSDB neuronal cell types in the presence of 100 nM kainate, intracellular recordings of MSDB neurones were made using sharp electrodes. The neurones were subdivided, according to criteria determined by previous studies, into slow firing (putative cholinergic) neurones and into burst firing, fast spiking and regular spiking (putative GABAergic) neurones. Burst firing neurones were distinguished from other neurone types by the fact that they display a burst of action potentials overlying a low threshold spike when given a depolarizing pulse at −75 mV but not at −60 mV (Griffith & Matthews, 1986; Griffith, 1988). Slow firing neurones were distinguished from the other cell types by their lack of depolarizing sag evident upon hyperpolarization (Gorelova & Reiner, 1996; Sotty *et al.* 2003). Fast spiking neurones were distinguished from regular spiking neurones by the relative lack of adaptation of the firing frequency of the former, exhibited during the application of long (600 ms) depolarizing pulses of different current magnitudes (Morris *et al.* 1999). Previous studies have suggested that the fast spiking cells of the MSDB are parvalbumin-positive GABAergic neurones and that the slow firing cells are cholinergic cells (Gorelova & Reiner, 1996; Morris *et al.* 1999; Knapp *et al.* 2000; Morris & Henderson, 2000; Sotty *et al.* 2003). We found that in areas where kainate-induced extracellular theta frequency activity could be recorded, regular firing neurones were not encountered, and burst firing neurones ($n = 3$) were rarely observed. We therefore concentrated on the properties of the slow firing ($n = 14$) and fast spiking neurones ($n = 16$) encountered. Combined recording and biocytin filling confirmed that the latter ($n = 4$) were a class of parvalbumin-containing neurones and that the slow firing cells ($n = 3$) did not contain parvalbumin (Fig. 7*A*).

During intracellular recordings the neurones, once characterized, were held at their resting membrane potentials and their spontaneous firing activity before and during bath application of 100 nM kainate was recorded and analysed. Fast spiking cells ($n = 11$) were spontaneously active at resting membrane potentials, and their spike interval decreased from 0.24 ± 0.11 s to 0.20 ± 0.13 s upon the application of 100 nM kainate (Fig. 7*Ca*). Slow-firing cells ($n = 9$), on the other hand, fired infrequently or at low frequency at resting membrane potentials, with an interspike interval of 0.87 ± 0.67 s. This decreased to 0.20 ± 0.13 s upon the application of 100 nM kainate (Fig. 7*Cb*). To investigate the firing activity patterns of MSDB neurones in relation to the kainate-induced extracellular theta activity, simultaneous recordings were made using sharp intracellular and extracellular field recordings (e.g. Fig. 7*B*). Spike-triggered averaging analysis of the firing activity of fast spiking and slow firing neurones was conducted *post hoc*. This demonstrated a high degree of coherence between the discharge of the fast spiking cell type and the trough of the theta cycle ($n = 5$; Fig. 7*Da*). The action potentials of the slow firing cell types were phase-locked to the peak of the theta cycle, thus firing 180 deg out of phase with the fast spiking cell type ($n = 5$; Fig. 7*Db*). Neither fast spiking nor slow firing neurones discharged within every single cycle of the extracellular theta activity (e.g. Fig. 7*B*).

Discussion

The results of this study suggest that the intrinsic circuitry of the MSDB is capable of generating and maintaining persistent network oscillatory activity at theta frequencies in the presence of kainate *in vitro*. Analysis of the underlying receptor mechanisms and the activity of different neuronal subtypes allowed the following main conclusions to be drawn: (i) $GABA_A$ receptor transmission, and possibly gap junctions, are required for the production of the theta frequency activity, whilst $GABA_B$ receptors only appear to have a modulatory role there; (ii) putative GABAergic and cholinergic neurone populations each display firing activity that is phase-locked to the rhythmic extracellular field activity. Thus coordinated activity of both the cholinergic and the GABAergic neurone populations seems to occur during generation of synchronized oscillatory activity at theta frequency in this *in vitro* model of the MSDB.

Synaptic mechanisms and evidence for network activity

Previously it has been shown that an essential component of synchronized network oscillatory activity in various areas of the brain is phasic synaptic activity based on the activation of $GABA_A$ receptors (review by Traub *et al.* 2004). The kainate-induced oscillatory activity in the MSDB was reduced or abolished by bicuculline and

that octanol abolishes the theta peak in the power spectrum. *H*, group data showing the percentage change in area power of the rhythmic activity for the putative gap junction antagonists tested. Asterisks indicate statistical significance for percentage change ($P < 0.05$). The error bars represent S.E.M.

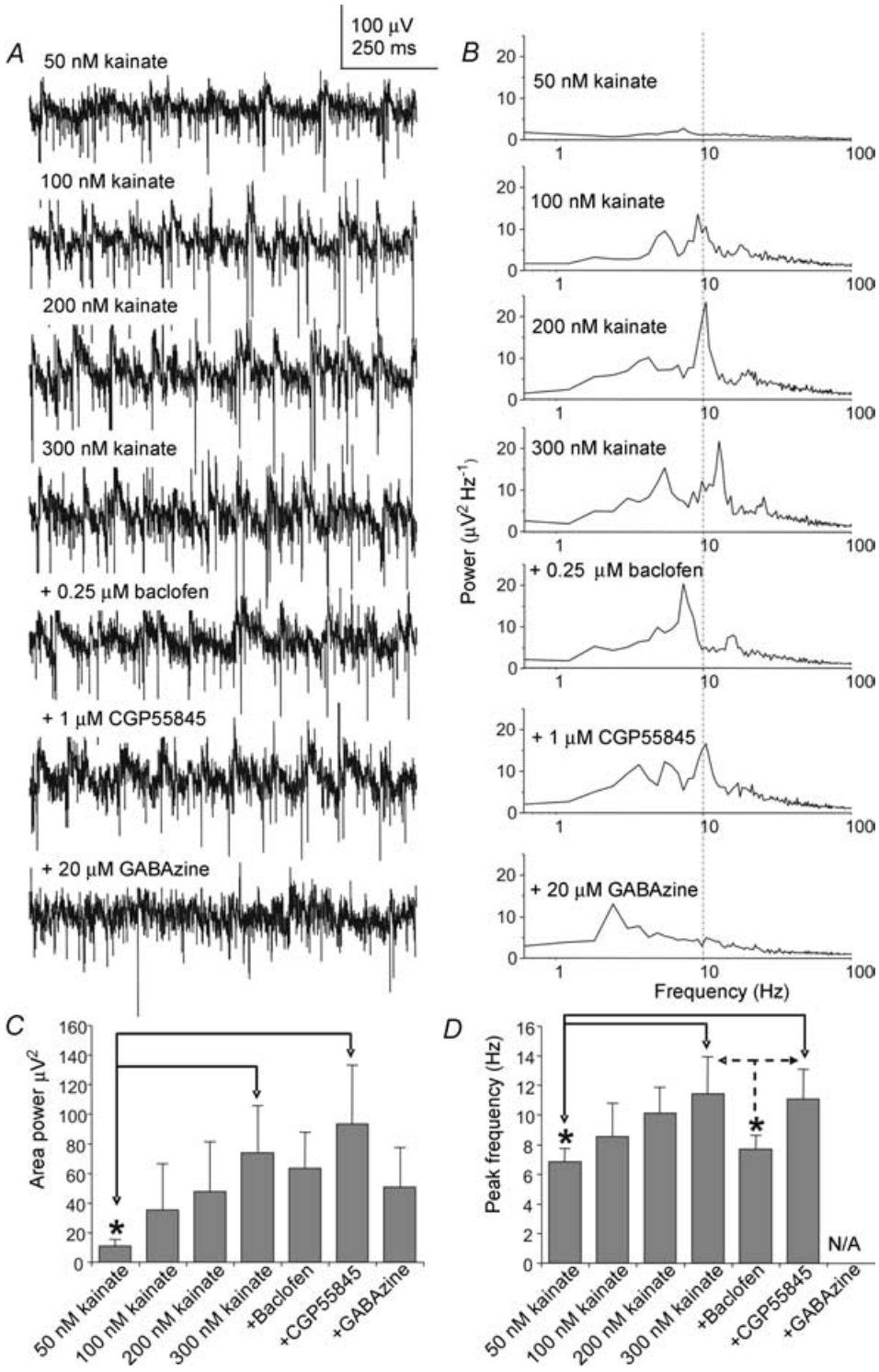

Figure 6. Characteristics of the extracellular theta field activity recorded in the MSDB slice in the presence of different concentrations of kainate at 37°C

A, example extracellular field recordings following application of increasing concentrations of kainate (50–300 nM), followed by 0.25 μM baclofen, then 1 μM CGP55845, and finally 20 μM GABAzine. *B*, example power spectra corresponding to the recordings in *A*, showing a gradual increase in the peak frequency of the oscillatory activity after addition of increasing concentrations of kainate. This is followed by a reduction of the frequency of the activity after addition of 0.25 μM baclofen, then counteraction of the effect following the addition of 1 μM CGP55845, and finally disruption of the theta field activity following the addition of 20 μM GABAzine. *C*, group data ($n = 3$ for GABAzine, and $n = 5$ for the other points), showing changes of area power in the presence of the agents tested

GABAzine, and was modulated by diazepam and by the activation of presynaptic $GABA_B$ receptors. Also, rhythmic compound IPSCs at theta frequency (5.9 ± 2.5 Hz, 30°C) have been recorded from the submerged MSDB slice in the presence of kainate, and the rhythmic compound IPSCs were modulated by baclofen in the same manner as the rhythmic extracellular field activity reported here (Henderson & Jones, 2005). Thus phasic $GABA_A$ receptor transmission appears to play a key role in the generation of the theta frequency population activity in the MSDB slice by kainate.

Although the extracellular oscillatory activity recorded in the MSDB was of relatively small amplitude compared with that recorded in the hippocampus (e.g. Hormuzdi *et al.* 2001), this was presumed to be due to the anatomical architecture of the MSDB in which dendrites, axon terminals and somata area are not organized into laminae as they are in the hippocampus. The kainate-induced oscillatory activity in the MSDB slice was localized preferentially in areas rich in parvalbumin-positive neurones confined to the midline part of the MSDB. Previously we have shown that this part of the MSDB is occupied by fast spiking, parvalbumin-containing cells interconnected by axosomatic synapses (Henderson *et al.* 2004). In cortical areas, these types of neurones are the key players in the production of synchronized network oscillatory activity (review by Freund, 2003). Thus the oscillatory activity described in the MSDB was most likely to have been mediated by mutual connections between the parvalbumin-containing GABAergic neurones in the midline part of the MSDB.

The mechanism of action of kainate at producing oscillatory activity in both the hippocampus and MSDB has yet to be determined. In the hippocampus, nanomolar concentrations of kainate have effects similar to that of micromolar concentrations of carbachol in producing network oscillatory activity. It has been suggested therefore that the kainate receptors in this situation provide a tonic excitatory input to the slice via metabotropic mechanisms (Traub *et al.* 2000). The kainate or carbachol-induced network oscillatory activity in the hippocampus requires the participation of interneurones and principal neurones, the latter via the phasic activation of AMPA receptors on the interneurones (review by Traub *et al.* 2004). Recently a local network of glutamatergic neurones has been described in the MSDB (Hajszan *et al.* 2004), although it is unknown whether this network was retained in the slice configuration used here. In our current study, we showed that kainate-induced theta frequency oscillations in the MSDB slice are blocked by the application of NBQX, but not by the NMDA receptor antagonist D-AP5. SYM 2206, a selective, non-competitive AMPA receptor antagonist (Li *et al.* 1999), abolishes certain components of rhythmic activity in the hippocampus and entorhinal cortex (Gillies *et al.* 2002; Cunningham *et al.* 2003), but had no significant effect on kainate-induced oscillatory activity in the MSDB. No conclusion about AMPA receptor participation can be drawn from this observation, however, because although AMPA/kainate receptor-based neurotransmission is present in the MSDB (Henderson & Jones, 2005), it was found to be relatively insensitive to the action of SYM 2206 (Z. Henderson, unpublished results). It should be mentioned though, that rhythmic compound EPSCs were not observed concurrently with the rhythmic compound IPSCs recorded in the submerged MSDB slice model used by Henderson & Jones (2005).

Kainate-induced oscillatory activity in the MSDB was not blocked by a non-selective antagonist of nicotinic receptors. The cholinergic neurones therefore do not appear to take the place of glutamatergic neurones in the provision of fast, phasic EPSPs during network oscillatory activity in the MSDB. This is in keeping with our previous electrophysiological studies indicating a lack of nicotinic receptor-based postsynaptic transmission in the MSDB (Henderson *et al.* 2005). Our previous anatomical studies have also indicated that the cholinergic neurones do not receive basket-like, parvalbumin-containing terminals on their somata (Henderson *et al.* 2004), as do the pyramidal cells in the hippocampus (Freund, 2003). This does not preclude the possibility, however, of the firing of the cholinergic neurones being influenced by axodendritic GABAergic terminals or by axosomatic GABAergic terminals that lack parvalbumin.

Gap junctions may play a role in the synchronization of oscillatory activity in the MSDB, as the rhythmic extracellular field activity was disrupted by the application of octanol or carbenoxolone, agents that have been shown to disrupt gamma frequency oscillations in the hippocampus (Traub *et al.* 2000; LeBeau *et al.* 2002). In the thalamus, synchronization of oscillatory activity in the theta frequency range seems to rely entirely on gap junctions, as demonstrated by the use of gap junctional modifying agents such as carbenoxolone, and also by other experimental approaches (Hughes *et al.* 2004). The actions of the pharmacological gap junction-blocking agents on their own do not provide sufficient evidence for the participation of gap junctions in the synchronization of oscillatory activity, and further confirmation of this in the

above. Significant differences between values are indicated by an asterisk ($P < 0.05$, ANOVA with Tukey's test). The error bars represent S.D. *D*, group data showing changes in frequency in the presence of the agents tested above. Significant differences between values are indicated by the asterisks ($P < 0.05$, ANOVA with Tukey's test). The error bars represent S.D.

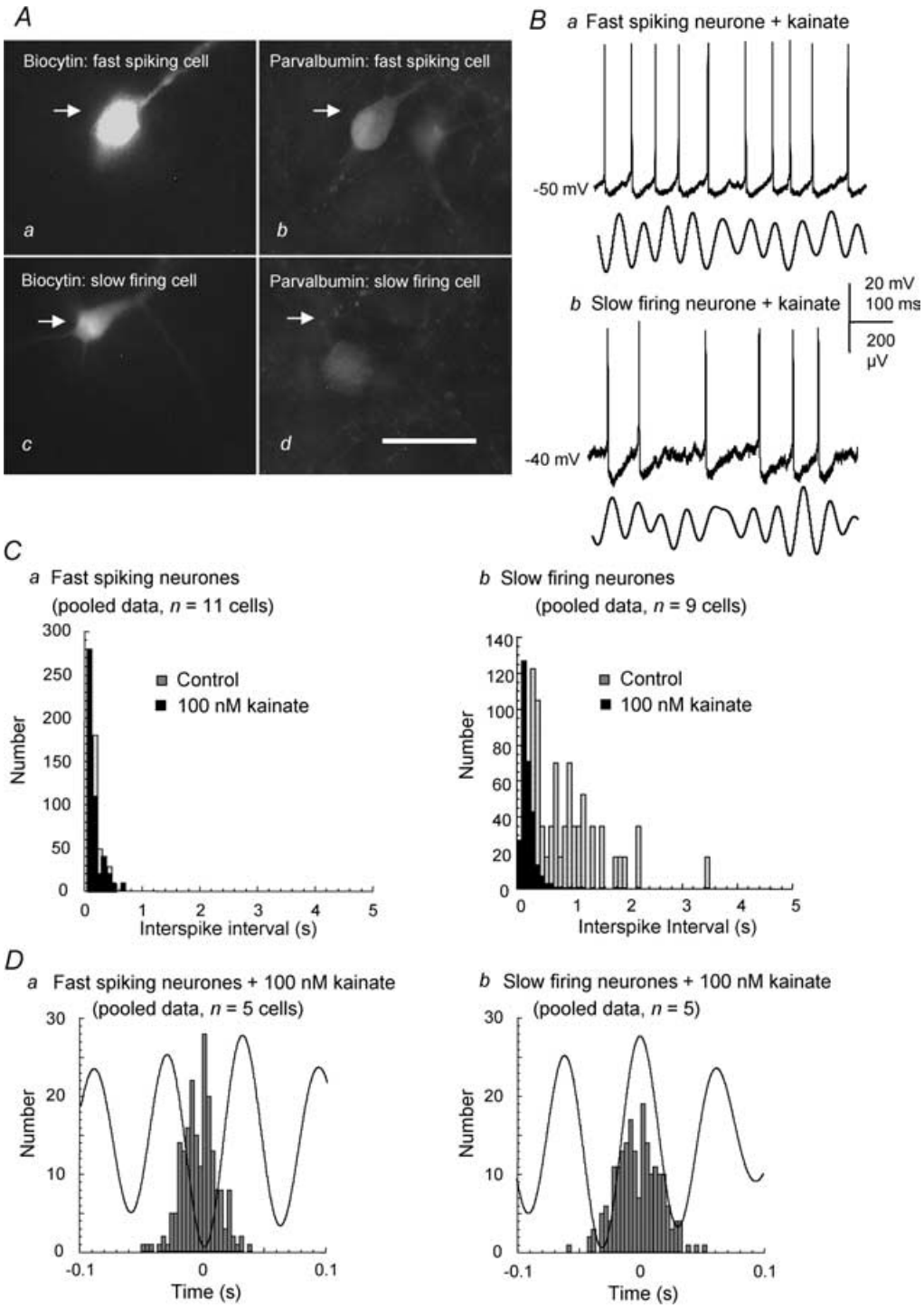

Figure 7. Characterization of the principal neurone types in the MSDB and their firing properties in the presence of kainate-induced oscillations

Aa–d, the cells were electrophysiologically characterized into fast spiking (putative GABAergic) or slow firing (putative cholinergic) according to previous published criteria. Subsequent biocytin-filling and immunohistochemistry confirmed that the fast spiking (*a* and *b*) and not the slow firing neurone (c and *d*) possesses parvalbumin immunoreactivity. Calibration bar, 50 μm. *Ba* and *b*, example traces of simultaneous intracellular recordings of spontaneous firing activity (upper traces) and extracellular field activity (lower traces; band pass filtered at 4–15 Hz) for a fast spiking (*Ba*) and a slow firing cell (*Bb*) in the presence of 100 nM kainate. *Ca*, interspike interval histogram demonstrating a slight increase in the firing rate and rhythmicity of the firing of a fast spiking neurone in the presence of kainate (pooled data from $n = 11$ cells). *Cb*, interspike interval histogram showing a more dramatic increase in the firing rate and rhythmicity of the firing of slow firing neurones in the presence

MSDB is required by other means (see Connors & Long, 2004). It is encouraging, nevertheless, that high levels of the mRNA of the neuronal gap junction protein connexin 36 are located in the MSDB in the postnatal days 24–60 rat brain (Belluardo *et al.* 2000).

Frequency of the oscillatory activity in the MSDB slice

Application of 50–300 nM kainate to the MSDB slice at 33°C and 37°C produced rhythmic extracellular field activity predominantly at theta frequency (4–12 Hz). Oscillatory activity recorded above this frequency range appeared not to be based on synaptic or network activity because it was not influenced by $GABA_A$ receptor blockers or by activation of presynaptic $GABA_B$ receptors. We could not be certain whether all the examples of oscillatory activity described in our experiments were truly representative of network population activity, because not all were tested with $GABA_A$ receptor blockers. In some cases this was impractical, for example, when mapping the distribution of kainate-induced rhythmic activity in the MSDB slice. It is notable that the application of a combination of nicotinic and muscarinic receptors led either to a complete or partial shift in the frequency of the oscillatory activity to that above the theta frequency range. The nature of the higher frequency activity was not tested with $GABA_A$ receptor blockers or baclofen, so it was not known whether the cholinergic inhibitors were disrupting network oscillatory activity or simply modulating the frequency of this activity.

The factors that govern the frequency of synchronized oscillations in inhibitory networks are not well understood. Computer simulation has shown that the postsynaptic conductance decay constants for $GABA_A$ IPSPs are suited for the generation of oscillatory activity in the gamma rather than the theta frequency band (Wang, 1993; Wang & Buzsaki, 1996). It has been suggested that an additional contribution of postsynaptic $GABA_B$ IPSPs is required for the generation of synchronization of activity at theta frequency (Wang & Rinzel, 1993). In the current study, however, we showed that the presence of $GABA_B$ receptors was not essential for the production of theta frequency oscillations in the MSDB. An alternate hypothesis is that 'slow' $GABA_A$ receptors are implicated in theta oscillations (Chapman & Lacaille, 1999; White *et al.* 2000). Recent simulation work in the hippocampus, on the other hand, has suggested that interneurone networks based on fast IPSPs are capable of generating highly coherent oscillations in a wide range of frequencies, including theta (Bartos *et al.* 2001; Traub *et al.* 2004).

Functional implications for the kainate-induced oscillatory activity in the MSDB slice

Septohippocampal neurones *in vivo* display a rhythmic bursting firing activity that is phase-locked with and tightly coupled to the frequency of hippocampal theta (Green & Arduini, 1954; Petsche *et al.* 1962; Apostol & Creutzfeldt, 1974; Alonso *et al.* 1987). Neurones that have rhythmic burst firing activity *in vivo* are confined to the midline MSDB (e.g. Sweeney *et al.* 1992; Borhegyi *et al.* 2004), so they most likely correspond to the neurones that produce single spiking activity that is phase-locked to the extracellular theta frequency activity produced by kainate in the MSDB slice. In our *in vitro* model we found the firing activities of both the GABAergic and cholinergic cells to be phase-locked with the extracellular field activity and 180 deg out of phase, which generally reflects the phase relation of the burst firing activity of GABAergic and cholinergic neurones *in vivo* (Brazhnik & Fox, 1997, 1999).

The generation of sustained rhythmic burst activity at theta frequency was not observed in our *in vitro* model, and has not been previously described in the MSDB slice (Griffith & Matthews, 1986; Griffith, 1988; Markram & Segal, 1990; Gorelova & Reiner, 1996; Morris *et al.* 1999; Henderson *et al.* 2001). The mechanism of generation of rhythmic burst firing *in vivo* remains unknown, although in GABAergic cells it does not appear to rely on phasic activity in reciprocal GABAergic connections (Brazhnik & Fox, 1997, 1999). The theta rhythm in the hippocampal formation *in vivo*, however, is highly sensitive to the injection of either $GABA_A$ receptor antagonists or atropine into the MSDB, actions which also eliminate the burst firing of the cholinergic cells (Brazhnik & Fox, 1997, 1999). Thus while the hippocampal theta rhythm does not rely entirely on rhythmic burst firing in the GABAergic neurones, it may require the synchronization or phase-locking of this burst firing activity, most likely via phasic GABAergic feedback modulated by a muscarinic cholinergic input (Brazhnik & Vinogradova, 1986; Lee *et al.* 1994). Atropine did not have any effect on the rhythmic activity produced in our preparation, but this is presumably because in our model the oscillatory activity was induced by the activation of kainate rather than muscarinic receptors.

In conclusion, our results on the effect of kainate on the MSDB slice may be relevant to the mechanisms responsible for the phase-locking of the rhythmic burst firing activity in the MSDB *in vivo*. The phase-locked rhythmic burst firing of septohippocampal neurones, would in turn, pace

of kainate (pooled data from $n = 9$ neurones). *Da*, spike-triggered-averaging analysis of the firing activity of fast spiking neurones, in the presence of kainate, shows that the neurones prefer to fire at the trough of the extracellular theta frequency oscillation (200 events; pooled data from $n = 5$ neurones). *Db*, spike-triggered-averaging analysis of the firing activity of slow firing neurones, in the presence of kainate, shows that the neurones prefer to fire at the peak of the extracellular theta frequency oscillation (200 events; pooled data from $n = 5$ neurones).

hippocampal interneurones preferably at theta rather than the gamma frequency at which the hippocampus naturally prefers to oscillate (Bragin *et al.* 1995; Cobb *et al.* 1995; Toth *et al.* 1997). The GABAergic circuitry in the MSDB that is responsible for the synchronization or phase-locking of rhythmic activity at theta frequency also appears to be dampened by the activation of presynaptic $GABA_B$ receptors, and this may come into force on occasions of intense activity *in vivo*, and it may be compromised by pathological situations.

References

Alonso A, Gaztelu JM, Buno W & Garcia-Austt E (1987). Cross-correlation analysis of septohippocampal neurons during theta-rhythm. *Brain Res* **413**, 135–146.

Apostol G & Creutzfeldt OD (1974). Crosscorrelation between the activity of septal units and hippocampal EEG during arousal. *Brain Res* **67**, 65–75.

Bartos M, Vida I, Frotscher M, Geiger JR & Jonas P (2001). Rapid signaling at inhibitory synapses in a dentate gyrus interneuron network. *J Neurosci* **21**, 2687–2698.

Belluardo N, Mudo G, Trovato-Salinaro A, Le Gurun S, Charollais A, Serre-Beinier V, Amato G, Haefliger JA, Meda P & Condorelli DF (2000). Expression of connexin 36 in the adult and developing rat brain. *Brain Res* **865**, 121–138.

Borhegyi Z, Varga V, Szilagyi N, Fabo D & Freund T (2004). Phase segregation of medial septal GABAergic neurons during hippocampal theta activity. *J Neurosci* **24**, 8470–8479.

Bragin A, Jando G, Nadasdy Z, Hetke J, Wise K & Buzsaki G (1995). Gamma (40–100-hz) oscillation in the hippocampus of the behaving rat. *J Neurosci* **15**, 47–60.

Brauer K, Seeger G, Hartig W, Rossner S, Poethke R, Kacza J, Schliebs R, Bruckner G & Bigl V (1998). Electron microscopic evidence for a cholinergic innervation of GABAergic parvalbumin-immunoreactive neurons in the rat medial septum. *J Neurosci Res* **54**, 248–253.

Brazhnik ES & Fox SE (1997). Intracellular recordings from medial septal neurons during hippocampal theta rhythm. *Exp Brain Res* **114**, 442–453.

Brazhnik ES & Fox SE (1999). Action potentials and relations to the theta rhythm of medial septal neurons in vivo. *Exp Brain Res* **127**, 244–258.

Brazhnik ES & Vinogradova OS (1986). Control of the neuronal rhythmic bursts in the septal pacemaker of theta-rhythm: effects of anaesthetic and anticholinergic drugs. *Brain Res* **380**, 94–106.

Buzsaki G (1989). Two-stage model of memory trace formation: a role for 'noisy' brain states. *Neuroscience* **31**, 551–570.

Chapman CA & Lacaille JC (1999). Intrinsic theta-frequency membrane potential oscillations in hippocampal CA1 interneurons of stratum lacunosum-moleculare. *J Neurophysiol* **81**, 1296–1307.

Cobb SR, Buhl EH, Halasy K, Paulsen O & Somogyi P (1995). Synchronization of neuronal activity in hippocampus by individual GABAergic interneurons. *Nature* **378**, 75–78.

Connors BW & Long MA (2004). Electrical synapses in the mammalian brain. *Ann Rev Neurosci* **27**, 393–418.

Cunningham MO, Davies CH, Buhl EH, Kopell N & Whittington MA (2003). Gamma oscillations induced by kainate receptor activation in the entorhinal cortex in vitro. *J Neurosci* **23**, 9761–9769.

Fisahn A, Pike FG, Buhl EH & Paulsen O (1998). Cholinergic induction of network oscillations at 40 Hz in the hippocampus in vitro. *Nature* **394**, 186–189.

Freund TF (1989). GABAergic septohippocampal neurons contain parvalbumin. *Brain Res* **478**, 375–381.

Freund TF (2003). Interneuron diversity series: Rhythm and mood in perisomatic inhibition. *Trends Neurosci* **26**, 489–495.

Freund TF & Antal M (1988). GABA-containing neurons in the septum control inhibitory interneurons in the hippocampus. *Nature* **336**, 170–173.

Frotscher M & Leranth C (1986). The cholinergic innervation of the rat fascia dentata: identification of target structures on granule cells by combining choline acetyltransferase immunocytochemistry and Golgi impregnation. *J Comp Neurol* **243**, 58–70.

Gillies MJ, Traub RD, LeBeau FEN, Davies CH, Gloveli T, Buhl EH & Whittington MA (2002). A model of atropine-resistant theta oscillations in rat hippocampal area CA1. *J Physiol* **543**, 779–793.

Gogolak G, Petsche H, Sterc J & Stumpf C (1967). Septum cell activity in the rabbit under reticular stimulation. *Brain Res* **5**, 508–510.

Gorelova N & Reiner PB (1996). Role of the afterhyperpolarization in control of discharge properties of septal cholinergic neurons in vitro. *J Neurophysiol* **75**, 695–706.

Green JD & Arduini AA (1954). Hippocampal electrical activity in arousal. *J Neurophysiol* **17**, 533–554.

Green KF & Rawlins JN (1979). Hippocampal theta in rats under urethane: generators and phase relations. *Electroencephalogr Clin Neurophysiol* **47**, 420–429.

Griffith WH (1988). Membrane properties of cell types within guinea pig basal forebrain nuclei in vitro. *J Neurophysiol* **59**, 1590–1612.

Griffith WH & Matthews RT (1986). Electrophysiology of AChE-positive neurons in basal forebrain slices. *Neurosci Lett* **71**, 169–174.

Gritti I, Mainville L & Jones BE (1993). Codistribution of GABA- with acetylcholine-synthesizing neurons in the basal forebrain of the rat. *J Comp Neurol* **329**, 438–457.

Hajszan T, Alreja M & Leranth C (2004). Intrinsic vesicular glutamate transporter 2-immunoreactive input to septohippocampal parvalbumin-containing neurons: Novel glutamatergic local circuit cells. *Hippocampus* **14**, 499–509.

Henderson Z, Boros A, Janzso G, Westwood AJ, Monyer H & Halasy K (2005). Somato-dendritic nicotinic receptor responses recorded in vitro from the medial septal diagonal band complex of the rodent. *J Physiol* **562**, 165–182.

Henderson Z, Fiddler G, Saha S, Boros A & Halasy K (2004). A parvalbumin-containing, axosomatic synaptic network in the rat medial septum: relevance to rhythmogenesis. *Eur J Neurosci* **19**, 2753–2768.

Henderson Z & Jones GA (2005). $GABA_B$ receptors in the medial septum/diagonal band slice from the 16–25 day rat. *Neuroscience* (in press).

Henderson Z, Morris NP, Grimwood P, Fiddler G, Yang HW & Appenteng K (2001). Morphology of local axon collaterals of electrophysiologically characterised neurons in the rat medial septal/diagonal band complex. *J Comp Neurol* **430**, 410–432.

Hormuzdi SG, Pais I, LeBeau FE, Towers SK, Rozov A, Buhl EH, Whittington MA & Monyer H (2001). Impaired electrical signaling disrupts gamma frequency oscillations in connexin 36-deficient mice. *Neuron* **31**, 487–495.

Hughes SW, Lorincz M, Cope DW, Blethyn KL, Kekesi KA, Parri HR, Juhasz G & Crunelli V (2004). Synchronized oscillations at alpha and theta frequencies in the lateral geniculate nucleus. *Neuron* **42**, 253–268.

Jones GA, Norris SK & Henderson Z (1999). Conduction velocities and membrane properties of different classes of rat septohippocampal neurons recorded in vitro. *J Physiol* **517**, 867–877.

Jouvet M (1969). Biogenic amines and the states of sleep. *Science* **163**, 32–41.

King C, Recce M & O'Keefe J (1998). The rhythmicity of cells of the medial septum/diagonal band of Broca in the awake freely moving rat: relationships with behaviour and hippocampal theta. *Eur J Neurosci* **10**, 464–477.

Kiss J, Patel AJ, Baimbridge KG & Freund TF (1990). Topographical localization of neurons containing parvalbumin and choline acetyltransferase in the medial septum-diagonal band region of the rat. *Neuroscience* **36**, 61–72.

Knapp JA, Morris NP, Henderson Z & Matthews RT (2000). Electrophysiological characteristics of non-bursting, glutamate decarboxylase messenger RNA-positive neurons of the medial septum/diagonal band nuclei of guinea-pig and rat. *Neuroscience* **98**, 661–668.

Kohler C, Chan-Palay V & Wu JY (1984). Septal neurons containing glutamic acid decarboxylase immunoreactivity project to the hippocampal region in the rat brain. *Anat Embryol* **169**, 41–44.

Lamour Y, Dutar P & Jobert A (1984). Septo-hippocampal and other medial septum-diagonal band neurons: electrophysiological and pharmacological properties. *Brain Res* **309**, 227–239.

Larson J & Lynch G (1986). Induction of synaptic potentiation in hippocampus by patterned stimulation involves two events. *Science* **232**, 985–988.

LeBeau FEN, Towers SK, Traub RD, Whittington MA & Buhl EH (2002). Fast network oscillations induced by potassium transients in the rat hippocampus in vitro. *J Physiol* **542**, 167–179.

Lee MG, Chrobak JJ, Sik A, Wiley RG & Buzsaki G (1994). Hippocampal theta activity following selective lesion of the septal cholinergic system. *Neuroscience* **62**, 1033–1047.

Lewis PR, Shute CC & Silver A (1967). Confirmation from choline acetylase analyses of a massive cholinergic innervation to the rat hippocampus. *J Physiol* **191**, 215–224.

Li P, Wilding TJ, Kim SJ, Calejesan AA, Huettner JE & Zhuo M (1999). Kainate-receptor-mediated sensory synaptic transmission in mammalian spinal cord. *Nature* **397**, 161–164.

Markram H & Segal M (1990). Electrophysiological characteristics of cholinergic and non-cholinergic neurons in the rat medial septum-diagonal band complex. *Brain Res* **513**, 171–174.

Morris NP, Harris SJ & Henderson Z (1999). Parvalbumin-immunoreactive, fast-spiking neurons in the medial septum/diagonal band complex of the rat: intracellular recordings in vitro. *Neuroscience* **92**, 589–600.

Morris NP & Henderson Z (2000). Perineuronal nets ensheath fast spiking, parvalbumin-immunoreactive neurons in the medial septum/diagonal band complex. *Eur J Neurosci* **12**, 828–838.

O'Keefe J & Conway DH (1978). Hippocampal place units in the freely moving rat: why they fire where they fire. *Exp Brain Res* **31**, 573–590.

Penttonen M, Kamondi A, Acsady L & Buzsaki G (1998). Gamma frequency oscillation in the hippocampus of the rat: intracellular analysis in vivo. *Eur J Neurosci* **10**, 718–728.

Petsche H, Stumpf C & Gogolák G (1962). The significance of the rabbit's septum as a relay station between the mid-brain and the hippocampus: the control of hippocampal arousal activity by septum cells. *Electroencephalogr Clin Neurophysiol* **14**, 202–211.

Singer W (1999). Neuronal synchrony: a versatile code for the definition of relations? *Neuron* **24**, 49–65.

Sotty F, Danik M, Manseau F, Laplante F, Quirion R & Williams S (2003). Distinct electrophysiological properties of glutamatergic, cholinergic and GABAergic rat septohippocampal neurons: novel implications for hippocampal rhythmicity. *J Physiol* **551**, 927–943.

Stewart M & Fox SE (1990). Do septal neurons pace the hippocampal theta rhythm? *Trends Neurosci* **13**, 163–168.

Sweeney JE, Lamour Y & Bassant MH (1992). Arousal-dependent properties of medial septal neurons in the unanesthetized rat. *Neuroscience* **48**, 353–362.

Toth K, Freund TF & Miles R (1997). Disinhibition of rat hippocampal pyramidal cells by GABAergic afferents from the septum. *J Physiol* **500**, 463–474.

Traub RD, Bibbig A, Fisahn A, LeBeau FEN, Whittington MA & Buhl EH (2000). A model of gamma-frequency network oscillations induced in the rat CA3 region by carbachol *in vitro*. *Eur J Neurosci* **12**, 4093–4106.

Traub RD, Bibbig A, LeBeau FEN, Buhl EH & Whittington MA (2004). Cellular mechanisms of neuronal population oscillations in the hippocampus in vitro. *Ann Rev Neurosci* **27**, 247–278.

Traub RD, Whittington MA, Colling SB, Buzsaki G & Jefferys JGR (1996). Analysis of gamma rhythms in the rat hippocampus in vitro and in vivo. *J Physiol* **493**, 471–484.

Vanderwolf CH (1969). Hippocampal electrical activity and voluntary movement in the rat. *Electroencephalogr Clin Neurophysiol* **26**, 407–418.

Vinogradova OS (1995). Expression, control, and probable functional significance of the neuronal theta-rhythm. *Prog Neurobiol* **45**, 523–583.

Wang XJ (1993). Ionic basis for intrinsic 40 Hz neuronal oscillations. *Neuroreport* **5**, 221–224.

Wang XJ & Buzsaki G (1996). Gamma oscillation by synaptic inhibition in a hippocampal interneuronal network model. *J Neurosci* **16**, 6402–6413.

Wang XJ & Rinzel J (1993). Spindle rhythmicity in the reticularis thalami nucleus: synchronization among mutually inhibitory neurons. *Neuroscience* **53**, 899–904.

White JA, Banks MI, Pearce RA & Kopell NJ (2000). Networks of interneurons with fast and slow gamma-aminobutyric acid type A ($GABA_A$) kinetics provide substrate for mixed gamma-theta rhythm. *Proc Natl Acad Sci U S A* **97**, 8128–8133.

Whittington MA, Traub RD & Jefferys JG (1995). Synchronized oscillations in interneuron networks driven by metabotropic glutamate receptor activation. *Nature* **373**, 612–615.

Wouterlood FG, Bol JGJM & Steinbusch HWM (1987). Double-label immunocytochemistry – combination of anterograde neuroanatomical tracing with phaseolus-vulgaris leukoagglutinin and enzyme immunocytochemistry of target neurons. *J Histochem Cytochem* **35**, 817–823.

Ylinen A, Soltesz I, Bragin A, Penttonen M, Sik A & Buzsaki G (1995). Intracellular correlates of hippocampal theta rhythm in identified pyramidal cells, granule cells, and basket cells. *Hippocampus* **5**, 78–90.

Acknowledgements

This work was supported by grants from the Wellcome Trust and the Medical Research Council of the UK (on which the late Professor E. H. Buhl had been coapplicant with Z.H., and principal applicant with M.A.W., respectively). H.L.G. was funded by a Biotechnology and Biological Sciences Research Council Studentship that had been held by Z.H. and Professor Buhl.